

Freezing of the local dynamics in the relaxor ferroelectric PZN-4.5%PT

Zhijun Xu,^{1,2} Jinsheng Wen,^{1,3} E. Mamontov,⁴ C. Stock,⁵ P. M. Gehring,⁶ and Guangyong Xu¹

¹*Condensed Matter Physics and Materials Science Department,
Brookhaven National Laboratory, Upton, New York 11973, USA*

²*Department of Physics, City College of New York, New York, New York 10033, USA*

³*Department of Materials Science and Engineering, Stony Brook University, Stony Brook, New York 11794, USA*

⁴*Neutron Scattering Science Division, Oak Ridge National Laboratory, Oak Ridge, Tennessee 37831, USA*

⁵*NIST Center for Neutron Research, National Institute of Standards and Technology, Gaithersburg,
Maryland 20899, and Indiana University Cyclotron Facility, Bloomington, Indiana 47404, USA*

⁶*NIST Center for Neutron Research, National Institute of Standards and Technology, Gaithersburg, Maryland 20899, USA*

(Dated: June 12, 2018)

We report measurements of the neutron diffuse scattering in a single crystal of the relaxor ferroelectric material 95.5%Pb(Zn_{1/3}Nb_{2/3})O₃-4.5%PbTiO₃ (PZN-4.5%PT). We show that the diffuse scattering at high temperatures has a quasielastic component with energy width $\gtrsim 0.1$ meV. On cooling the total diffuse scattering intensity increases, but the intensity and the energy width of the quasielastic component gradually diminish. At 50 K the diffuse scattering is completely static (i. e. the energy width lies within the limits of our instrumental resolution). This suggests that the dynamics of the short-range correlated atomic displacements associated with the diffuse scattering freeze at low temperature. We find that this depends on the wave vector q as the quasielastic diffuse scattering intensities associated with $\langle 001 \rangle$ (T1-type) and $\langle 110 \rangle$ (T2-type) atomic displacements vary differently with temperature and electric field.

PACS numbers: 77.80.Jk, 77.84.-s, 28.20.Cz

I. INTRODUCTION

The physics of lead-based, perovskite, relaxor systems (PbBO₃), such as Pb(Zn_{1/3}Nb_{2/3})O₃ (PZN), and Pb(Mg_{1/3}Nb_{2/3})O₃ (PMN), are complicated by the random fields generated by the charge disorder on the B-site. Nanometer-scale polar clusters, or “polar nano-regions” (PNRs), are widely believed to form at the Burns temperature T_d ,¹ which is typically a few hundred degrees above the Curie temperature T_C . Many unusual bulk properties of relaxor systems have been attributed to these PNRs²⁻⁶, and consequently they have been the focus of extensive study. Various models of the short-range correlated (i. e. local) atomic displacements that define the PNRs have been proposed based on extensive neutron and x-ray scattering studies of these and other related relaxor systems.⁷⁻¹⁴ Our most recent work¹⁵ shows that the diffuse scattering measured in a specific region of reciprocal space varies strongly in the presence of an electric field \mathbf{E} oriented along $[111]$, but not for \mathbf{E} oriented along $[100]$, while the opposite behavior is observed for the diffuse scattering measured in a nearby region of reciprocal space. This suggests that the local atomic displacements comprising the PNRs may be composed of two distinct components that give rise to two distinct, but overlapping, diffuse scattering distributions that are located near every Brillouin zone center. In our model the local atomic displacements along $\langle 110 \rangle$ are responsible for the well-known butterfly-shaped diffuse scattering,^{7,16-20} which responds strongly to \mathbf{E} along $[111]$; we then speculate that local atomic displacements along $\langle 001 \rangle$ could produce a differently shaped diffuse scattering distribution that would instead respond strongly to \mathbf{E} along $[100]$. Following previously defined nomenclature, we shall refer to the first as T2-diffuse scattering because of its similarity to T2 transverse acoustic (TA) phonon modes, which are polarized

along $\langle 110 \rangle$,⁶ and we shall refer to the second as T1-diffuse scattering by analogy to T1 phonon modes, which are polarized along $\langle 001 \rangle$.²¹

Scattering methods are essential tools for mapping out the wave vector (\mathbf{Q}) dependence of the diffuse scattering in relaxors, which in turn provides key structural information about the atomic displacements associated with the PNRs as well as the length scales over which these displacements are correlated. One can also obtain information about the energy/time scales associated with the PNRs. Neutron-based methods can easily distinguish between static and thermal diffuse scattering. However, depending on the temperature, the diffuse scattering from the PNRs can exhibit both elastic and quasielastic components; this has been conclusively demonstrated by neutron measurements made with very high energy resolution.^{4,15,18,22,23} Recent neutron spin echo measurements have shown that the PNRs in both PMN and the related relaxor system PZN-4.5%PT (a solid solution of PZN and PbTiO₃) display relaxational dynamics at high temperatures with a typical lifetime of around 0.0042 ns, which corresponds to an energy width of 0.16 meV. These dynamic, local structures gradually freeze on cooling and become entirely static at sufficiently low temperatures.

In this paper, we discuss detailed measurements of the T1- and T2-diffuse scattering components made simultaneously on the same single crystal of PZN-4.5%PT. We find that the dynamics of both components follow the same trend - freezing with cooling. One difference is that the T1-component exhibits a narrower energy width, i. e. a longer life time, than does the T2-component measured at the same temperature. An external field applied along $[001]$ does not affect the T2-component, but it significantly reduces the intensity of the T1-component near T_C . These results confirm that subtle differences exist between the dynamics of PNRs measured at two

different wave vectors within the same Brillouin zone and lend support to the concept that the PNRs are composed of two distinct components. Possible connections between the local dynamics and bulk lattice dynamics (phonons) are discussed.

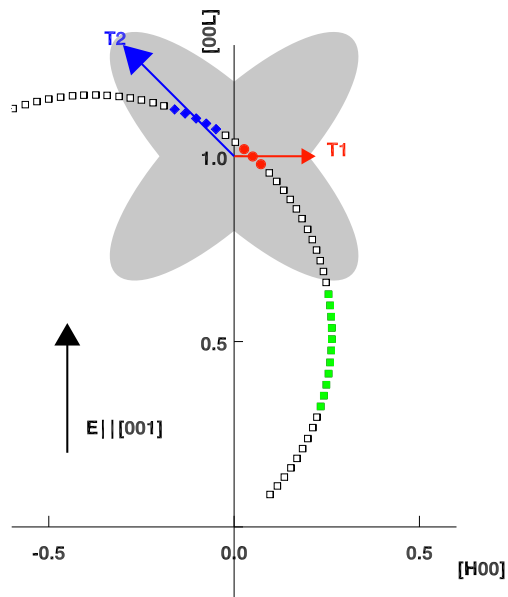


FIG. 1: (Color online) Schematic diagram of the scattering geometry in which measurements were made in the (HOL) plane with an electric field applied along [001]. The grey butterfly-shaped region represents constant-intensity contours of the T2-diffuse scattering centered at $\mathbf{Q}=(0,0,1)$. The small squares show the locations in \mathbf{Q} of the BASIS detectors for elastically ($\hbar\omega = 0$) scattered neutrons.

II. EXPERIMENTAL DETAILS

The sample studied in this experiment is a rectangular single crystal of PZN-4.5%PT with $\{100\}$ surfaces and dimensions of $10 \times 10 \times 3 \text{ mm}^3$. The sample has a cubic lattice spacing of $a = 4.05 \text{ \AA}$ at 300 K; thus 1 r.l.u. (reciprocal lattice unit) equals $2\pi/a = 1.55 \text{ \AA}^{-1}$. Cr/Au electrodes were sputtered onto the two largest opposing crystal surfaces. The Curie temperature of this compound $T_C \sim 475 \text{ K}$. This is manifested by a release of extinction that results in a more than two-fold increase in the intensity of the (100) Bragg peak on cooling.¹⁵

Neutron diffuse scattering measurements were performed on the BASIS backscattering spectrometer, which is located at the Oak Ridge National Laboratory Spallation Neutron Source (SNS). A large bank of Si(111) crystals is employed as analyzer to reflect those neutrons scattered by the sample that have a final energy of $E_f=2.082 \text{ meV}$. The incident neutron energy bandwidth is centered around the same energy using a series of bandwidth choppers. The instrumental energy resolution is about 1.5 \mu eV half-width at half-maximum (HWHM) for elastically ($\hbar\omega = 0$) scattered neutrons. The a -axis of the

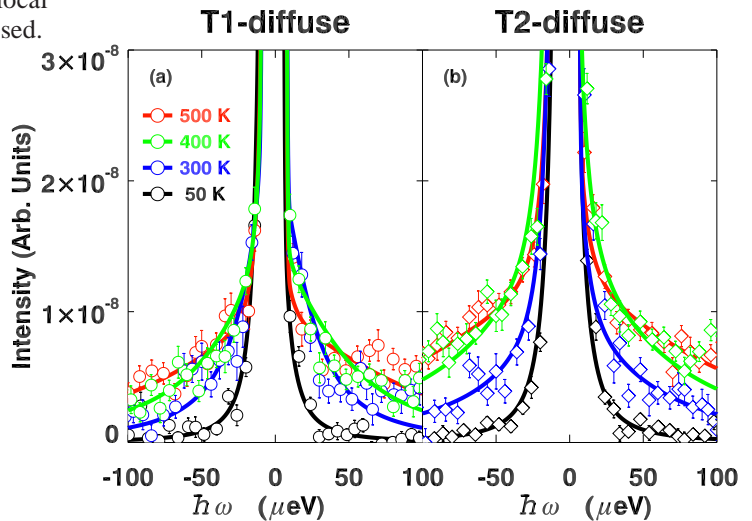


FIG. 2: (Color online) Diffuse scattering intensities are plotted versus $\hbar\omega$ at 500 K (red), 400 K (green), 300 K (blue), and 50 K (black) for the (a) T1-component, measured at $\mathbf{Q} = (0.05, 0, 1)$, and the (b) T2-component, measured at $\mathbf{Q} = (-0.1, 0, 1.1)$. The solid lines are based on the least square fits to the data described in the text. The error bars represent the square root of the number of counts.

crystal was aligned so that it formed a 54° angle with respect to the incident beam. In this configuration the BASIS detectors collected quasielastic scattering (i. e. centered around $\hbar\omega = 0$) intensities at the reciprocal space locations shown in Fig. 1. Given the large detector coverage provided by BASIS we were able to measure the diffuse scattering intensities at many different \mathbf{Q} values at the same time. Our measurements show that this spectrometer is well-suited to the study of quasielastic scattering in the μeV energy range from single crystal samples. An external electric field $E = 1 \text{ kV/cm}$ was applied along [001] above 550 K during all of the field-cooled (FC) measurements.

III. RESULTS AND DISCUSSION

We performed a series of measurements to characterize the dynamics of the diffuse scattering in the (HOL) plane under different temperatures and field-cooling conditions. Based on the area detector design of BASIS, the group of detectors marked in blue in Fig. 1 were summed to give the intensity in a small neighborhood of $\mathbf{Q} = (-0.10, 0, 1.10)$, which corresponds to the T2-component. Similarly the group of detectors shown in red should reflect intensities near $\mathbf{Q} = (0.05, 0, 1)$, which corresponds to the T1-component. The group of detectors shown in green are located far enough from the Bragg peak that they may be summed and used to measure the background; the intensities collected by this group of detectors ex-

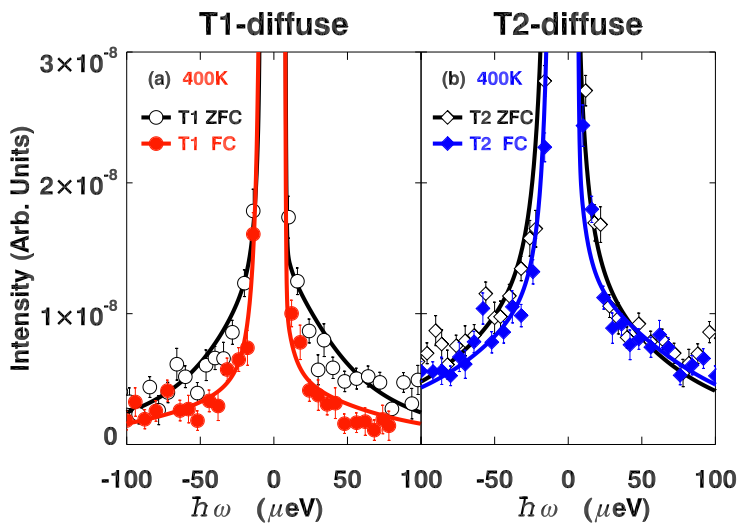


FIG. 3: (Color online) Diffuse scattering intensities are plotted versus $\hbar\omega$ at 400 K after zero-field cooling (ZFC: black, open symbols) and field cooling (FC: red, solid symbols). Data are shown for the (a) T1-component, measured at $\mathbf{Q} = (0.05, 0, 1)$, and the (b) T2-component, measured at $\mathbf{Q} = (-0.1, 0, 1.1)$. The solid lines are based on the least square fits to the data described in the text. The error bars represent the square root of the number of counts.

hibited no measurable \mathbf{Q} or temperature dependence.

The T1 diffuse scattering intensities measured by the red detectors are plotted in panel (a) of Fig. 2 after first subtracting out the background intensities collected by the green detectors. At 50 K the diffuse scattering lineshape is resolution-limited; hence all quasielastic processes occurring on instrumentally-accessible time scales are frozen. These data are well-described by the sum of a Gaussian and Lorentzian function of energy, and they represent the total (static) scattering response of the system, which is composed of the static diffuse scattering plus any incoherent scattering. This curve is slightly asymmetric as explained in Ref. 24, and was then used to model the instrumental energy resolution function at all temperatures. Data measured above 50 K were fit to the same Gaussian and Lorentzian functions times an overall scale factor, and then added to another Lorentzian function that was used to parameterize the quasielastic component. The T2-diffuse scattering intensities are plotted in panel (b) of Fig. 2; the fittings for these data were performed in the same manner as done for the T1-component data.

On cooling quasielastic scattering from both the T1- and T2-components appears at temperatures well above T_C . At 500 K both components display slow dynamics characterized by HWHM energy widths of $\hbar\Gamma(T1) \sim 0.09(\pm 0.005)$ meV and $\hbar\Gamma(T2) 0.11(\pm 0.005)$ meV. These values are in reasonably good agreement with those determined by our recent spin-echo measurements.^{15,23} At lower temperatures both en-

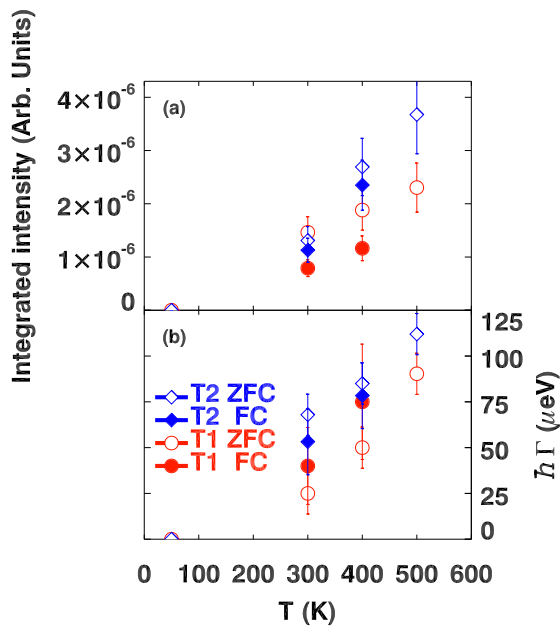


FIG. 4: (Color online) (a) Energy width $\hbar\Gamma$ (half width at half maximum) of the quasielastic diffuse scattering versus temperature for the T1-component (ZFC = red, open circles; FC = red, solid circles) and the T2-component (ZFC = blue, open diamonds; FC = blue, solid diamonds). (b) Temperature dependence of the integrated intensities of the quasielastic diffuse scattering.

ergy widths narrow, as shown in panel (b) of Fig. 4. The quasielastic scattering intensity also decreases monotonically from 500 K to 300 K. Near 50 K the diffuse scattering becomes entirely static. We note that for all temperatures studied, the energy widths $\Gamma(T1) < \Gamma(T2)$, which suggests that subtle differences exist between the local dynamics associated with $\langle 001 \rangle$ and $\langle 110 \rangle$ oriented atomic displacements. At a given temperature the T2-component exhibits a shorter lifetime, but at sufficiently low temperatures both are entirely static.

The integrated intensity of the quasielastic scattering associated with both the T1- and T2-components (see panel (a) of Fig. 4) also decreases on cooling, whereas the total diffuse scattering intensity increases. This confirms that the PNRs become increasingly longer-lived as the temperature is lowered. The quasielastic scattering intensity of the T2-component is clearly stronger than that of the T1-component, even though the T2-component intensities are being measured at an average wave vector located further from the Bragg peak. We thus conclude that the T2-component is the dominant contribution to the diffuse scattering intensities.

We have also examined the effects of an external electric field on the quasielastic components of the T1- and T2-diffuse scattering. As can be seen from panel (b) of Fig. 3, essentially no change in the T2-component is observed when the system is cooled from 550 K to 400 K in a 1 kV/cm electric field applied along $[001]$. This result is consistent with our previous observations.^{15,25} By contrast, the data in panel (a) of Fig. 3

demonstrate that the same field greatly affects (reduces) the T1-component. In order to characterize these observations in greater detail, the integrated intensities and the energy widths (HWHM) of the two quasielastic components were extracted from fits to the total diffuse scattering as previously described. These quantities are plotted as a function of temperature in Fig. 4 for both ZFC and FC conditions. We emphasize that the [001] field direction is parallel to the direction of the local atomic displacements that are associated with the T1-diffuse scattering measured near $\mathbf{Q} = (001)$. As expected, these data show that the quasielastic component of the T1-diffuse scattering intensity is significantly weakened by the [001] electric field, but that the same is not true for the T2-component.¹⁵ The energy widths associated with each component, on the other hand, have such large uncertainties that no conclusion can be drawn about the respective electric field dependence. For example, at 400 K the field-cooled quasielastic energy width of the T1-component appears to be enhanced relative to the zero-field cooled case, but the difference between the two lies within our experimental error. On cooling to 300 K the field effects appear to become less pronounced, but this trend also lies within our experimental uncertainties.

Our finding that the dynamics associated with the T1-component are slower than those associated with the T2-component may be understood when interactions between the acoustic phonons and the PNRs are taken into consideration. Normally T2 phonons are softer than T1 phonons in PZN- x %PT and PMN- x %PT relaxors that exhibit a rhombohedral ground state.²⁶ Previous work has conclusively shown that whereas the relaxational T2-diffuse scattering couples strongly to TA2 phonons,^{6,27,28} the coupling between the relaxational T1-diffuse scattering and the TA1 phonons is weaker²⁸. There are, however, also indications of a coupling between the T1-diffuse and TO1 optic phonons.²⁹ In other words, the local atomic displacements within the PNRs can be affected by phonons provided that they share the same polarization; these then induce slow, local modes within the PNRs, which give rise to the quasielastic scattering that are discussed in this paper. Along $\langle 110 \rangle$ where the bulk phonons are softer

and the coupling is stronger, the local atomic displacements become more dynamic and therefore the quasielastic component of the T2-diffuse scattering could have a larger energy width. Our finding thus adds an important, new piece of information to the already puzzling picture of competing and co-existing local and long-range polar order in relaxor systems³⁰ and deserves further study.

IV. SUMMARY

We have characterized the temperature and field dependence of the quasielastic diffuse scattering measured from a single crystal sample of the relaxor ferroelectric PZN-4.5%PT using neutron backscattering, which provides excellent energy resolution. Our data show that both the T1- and T2-components of the diffuse scattering exhibit quasielastic character at high temperatures that diminishes gradually on cooling. We also observe differences between the dynamics of these two components, which provides further evidence that, in addition to the well-known and more extensively studied T2-component, a distinct, weaker, and lesser known T1-component is also present, which is associated with local atomic displacements along $\langle 001 \rangle$. Given that the T2-component has already been shown to affect the polar properties of this relaxor system, it is quite possible that the T1-component does so as well. It thus merits study in much greater detail in the future.

V. ACKNOWLEDGMENTS

Financial support from the US Department of Energy under contract No. DE-AC02-98CH10886 is gratefully acknowledged. This research at the Oak Ridge National Laboratory Spallation Neutron Source was sponsored by the Scientific User Facilities Division, Office of Basic Energy Sciences, U. S. Department of Energy.

¹ G. Burns and F. H. Dacol, Phys. Rev. B **28**, 2527 (1983).

² L. E. Cross, Ferroelectrics **76**, 241 (1987).

³ B. P. Burton, E. Cockayne, S. Tinte, and U. V. Waghmare, Phase Transitions: A Multinational Journal **79**, 91 (2006).

⁴ P. M. Gehring, H. Hiraka, C. Stock, S. H. Lee, W. Chen, Z. G. Ye, S. B. Vakhrushev, and Z. Chowdhuri, Phys. Rev. B **79**, 224109 (2009).

⁵ M. Matsuura, K. Hirota, P. M. Gehring, Z.-G. Ye, W. Chen, and G. Shirane, Phys. Rev. B **74**, 144107 (2006).

⁶ G. Xu, J. Wen, C. Stock, and P. M. Gehring, Nature Mater **7**, 562 (2008).

⁷ G. Xu, Z. Zhong, Y. Bing, Z. G. Ye, and G. Shirane, Nature Mater **5**, 134 (2006).

⁸ G. Xu, Z. Zhong, H. Hiraka, and G. Shirane, Phys. Rev. B **70**, 174109 (2004).

⁹ T. R. Welberry, M. J. Gutmann, D. H. Woo, J. Goossens, G. Xu, C. Stock, W. Chen, and Z.-G. Ye, J. appl. cryst. **38**, 639 (2005).

¹⁰ T. R. Welberry, D. J. Goossens, and M. J. Gutmann, Phys. Rev. B **74**, 224108 (2006).

¹¹ A. Cervellino, S. Gvasaliya, O. Zaharko, B. Roessli, G. Rotaru, R. Cowley, S. Lushnikov, T. Shaplygina, and M.-T. Fernandez-Diaz, arXiv:0908.2920v2 (2009).

¹² I. K. Jeong, T. W. Darling, J. K. Lee, T. Proffen, R. H. Heffner, J. S. Park, K. S. Hong, W. Dmowski, and T. Egami, Phys. Rev. Lett. **94**, 147602 (2005).

¹³ S. B. Vakhrushev, A. A. Naberezhnov, N. M. Okuneva, and B. N. Savenko, Phys. Solid State **37**, 1993 (1995).

¹⁴ K. Hirota, Z. G. Ye, S. Wakimoto, P. M. Gehring, and G. Shirane, Phys. Rev. B **65**, 104105 (2002).

¹⁵ Z. Xu, J. Wen, G. Xu, C. Stock, J. S. Gardner, and P. M. Gehring, Phys. Rev. B **82**, 134124 (2010).

¹⁶ H. You and Q. M. Zhang, Phys. Rev. Lett. **79**, 3950 (1997).

¹⁷ J. Hlinka, S. Kamba, J. Petzelt, J. Kulda, C. A. Randall, and S. J. Zhang, J. Phys. Condens. Matter **15**, 4249 (2003).

- ¹⁸ H. Hiraka, S. H. Lee, P. M. Gehring, G. Xu, and G. Shirane, *Phys. Rev. B* **70**, 184105 (2004).
- ¹⁹ G. Xu, Z. Zhong, Y. Bing, Z.-G. Ye, C. Stock, and G. Shirane, *Phys. Rev. B* **70**, 064107 (2004).
- ²⁰ C. Stock, G. Xu, P. M. Gehring, H. Luo, X. Zhao, H. Cao, J. F. Li, D. Viehland, and G. Shirane, *Phys. Rev. B* **76**, 064122 (2007).
- ²¹ P. M. Gehring, K. Ohwada, and G. Shirane, *Phys. Rev. B* **70**, 014110 (2004).
- ²² S. N. Gvasaliya, S. G. Lushnikov, and B. Roessli, *Phys. Rev. B* **69**, 092105 (2004).
- ²³ C. Stock, L. Van Eijck, P. Fouquet, M. Maccarini, P. M. Gehring, G. Xu, H. Luo, X. Zhao, J. F. Li, and D. Viehland, *Phys. Rev. B* **81**, 144127 (2010).
- ²⁴ E. Mamontov and K. W. Herwig, *Rev. Sci. Instrum.* **82**, 085109 (2011).
- ²⁵ J. Wen, G. Xu, C. Stock, and P. M. Gehring, *Appl. Phys. Lett.* **93**, 082901 (2008).
- ²⁶ I. P. Swainson, C. Stock, P. M. Gehring, G. Xu, K. Hirota, Y. Qiu, H. Luo, X. Zhao, J. F. Li, and D. Viehland, *Phys. Rev. B* **79**, 224301 (2009).
- ²⁷ C. Stock, H. Luo, D. Viehland, J. F. Li, I. P. Swainson, R. J. Birgeneau, and G. Shirane, *J. Phys. Soc. Jpn.* **74**, 3002 (2005).
- ²⁸ C. Stock, et al., unpublished .
- ²⁹ Z. Xu, et al., unpublished .
- ³⁰ G. Xu, P. M. Gehring, and G. Shirane, *Phys. Rev. B* **74**, 104110 (2006).